4n+2=6n?

Aristides D. Zdetsis*

Molecular Engineering Laboratory, Department of Physics, University of Patras, Patras 26500 GR, Greece, and

Institute of Electronic Structure and Laser, Foundation for Research &Technology Hellas, Vassilika Vouton, P.O. Box 1385, Heraklion, Crete GR-71110, Greece

ABSTRACT

Using a simple, insightful but powerful geometrical/topological notion of aromaticity, emphasizing the closer interrelation/equivalence between Hückel's and Clar's fundamental rules, we can "redesign" various nanographenes with drastically improved electronic and structural characteristics, verifying at the same time the dominant role of aromaticity for graphene and nanographene(s), and in particular the role of the "empty" (non-aromatic) peripheral rings in conjunction with zigzag bonding. Thus, manipulating empty peripheral rings (e.g. with the STM tip) we can manipulate bandgaps, spin or pseudospin, sublattice imbalance, as well as topological edge/end-states. Removing empty (non-aromatic) peripheral rings in hexagonal zigzag nanographenes, corresponding to π-electrons of "balanced" symmetry and parity, is shown to lead to "equivalent" (electronically/aromatically) armchair structures with much larger gaps. Partial elimination under D_{3h} subgroup symmetry leads to armchair triangular nanographenes, with no real Dirac points, having only one (Clar/Hückel-type) aromaticity pattern, regardless parity and π-electron number, due to lack of molecular-sublattice-symmetry conflict. Moreover, applying the same "truncation" strategy to zigzag triangular nanographenes (triangulenes), which due to sublattice imbalance are unstable, topologically frustrated with high spin states, is shown to relieve sublattice imbalance and reduce spin (by 3 units), leading to more stable or even naturally abundant structures. The paradigms of hexabenzocoronene, and 1,3,5-

triphenylbenzene among others, are highly suggestive that such process could be natural, not just conceptual, or mechanical. Therefore, we propose a unique scheme to manipulate in a coordinated way chemically or mechanically topological, aromatic, electronic, and magnetic (conventional or non-conventional) properties of various nanographenes simultaneously. This could be very useful for nanoelectronics and spintronics applications.

*zdetsis@upatras.gr

TOC Graphic

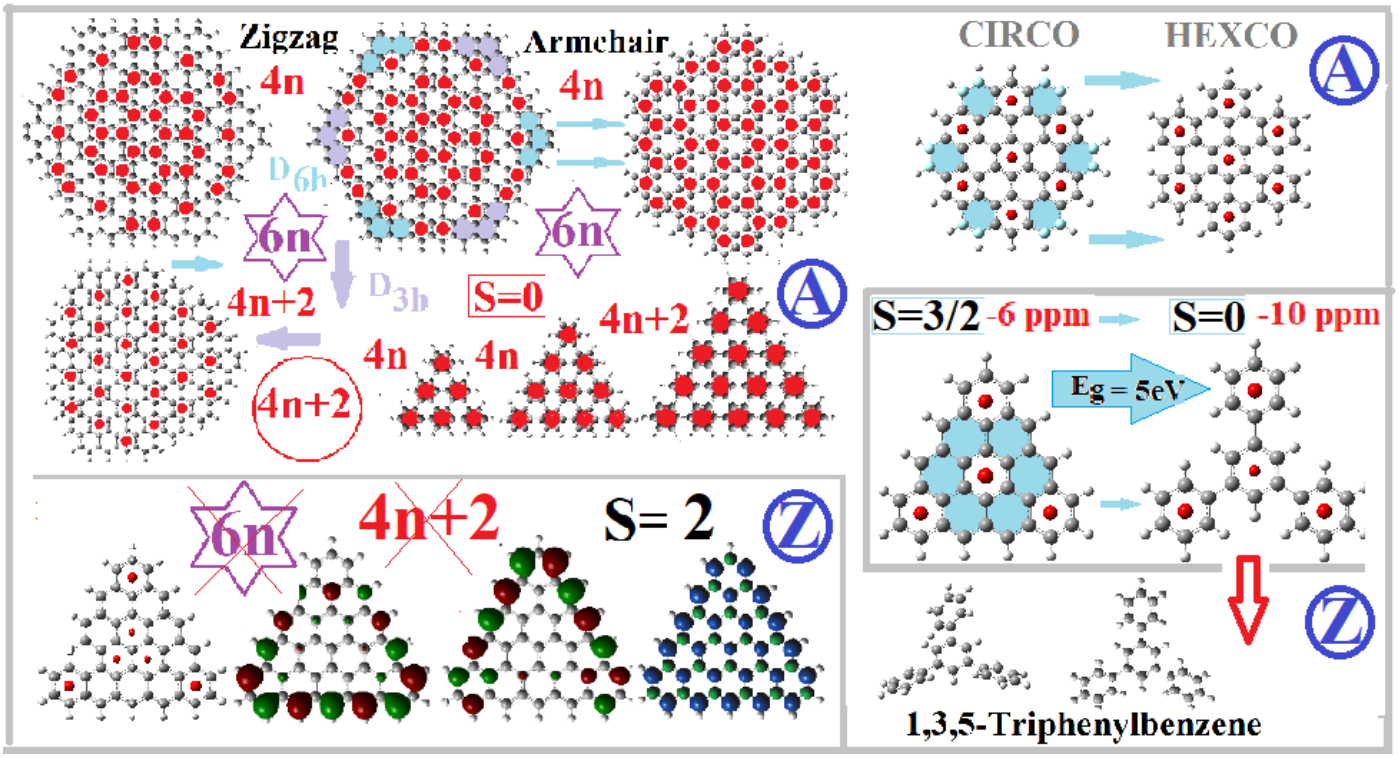

Highlights

- **Hückel's and Clar's Fundamental rules of aromaticity are not independent and sometimes coincide,**
- **Resulting in close interrelationship of empty non-aromatic peripheral rings with zigzag (peripheral) bonds**
- **Eliminating non-aromatic peripheral rings in hexagonal zigzag NGRs leads to armchair NGRs with improved properties**
- **Partial symmetrical elimination leads to triangular armchair NGRs, with no Dirac points, fully satisfying Clar's rules, independently of size**
- **Applying this strategy to triangulenes leads to more stable (sometimes naturally abundant), less-frustrated, lower- spin structures.**
- **Based on paradigms of hexabenzocoronene and triphenylbenzene, it is suggested that this could be a natural (not just a conceptual or mechanical) process**

1. Introduction. The molecular approach of graphene through a sequence of growing size polycyclic aromatic hydrocarbons (PAHs) has been recently proven very successful and insightful, deciphering at the molecular level all or most of the "exotic" properties of graphene, pinpointing their deeper roots and origins, and providing at the same time totally new information and interpretation(s),[1-3] revealing that graphene is the analogous crystalline prototypical aromatic solid in full analogy to the prototypical aromatic molecule of benzene[2]. The new emerging feature is the dominant role of aromaticity (in all of its forms, expressions and manifestations), combined with topology and symmetry, involved in the molecular versus (sub)lattice symmetry competition, which is responsible for the chiral character of graphene and the driving force behind its exotic properties. These key properties are all interrelated in known and unknown, but mostly indirect ways, which are here revealed in a one-to-one correspondence; Thus allowing to pinpoint particular individual rings, responsible for particular electronic and aromatic characteristics (for example "empty" peripheral rings associated with specific zigzag bonds). This is shown here to lead to guided molecular engineering, analogous to the pioneering synthesis of 3-triangulene, using the tip of a scanning tunnelling microscope (STM) to physically move individual atoms[4] and rings. Although the present (theoretical) methodology can (and do, as will be shown below) help to substantially relief the sublattice imbalance, which is responsible for the violation of the well-known of Kekulé bonding rules, the primary target is to significantly improve the electronic, aromatic, and structural properties of much less unstable structures, such as nanographenes (NGRs). This is accomplished by improving, combining, and re-interpreting the fundamental aromaticity rules of Hückel (4n+2) and Clar (6n), which reflect Kekulé's bonding rules. Yet, unstable (highly reactive) structures which violate Kekulé's, such as various triangulenes[5-6] and other

"elusive" structures[7] have been recently synthesized using novel bottom up atomically precise techniques, employing suitable precursors on metallic substrates. Obviously, such structures violate Kekulé rules and inversion symmetry requirements, which are directly connected with chirality. On the other hand, inversion symmetry competition (in the proper topological framework) is very constructive for NGRs, PAHs, and graphene itself, leading to Dirac points and topological end/edge states or other novel properties. In this work specifically, we uncover and demonstrate a few basic principle(s) for guided molecular (or rather ring) engineering, which allows among others for the successful and promising transformation of zigzag structures to armchair ones with improved properties such as aromaticity, and energy gaps (such as between highest occupied and lowest unoccupied molecular orbitals, HOMO and LUMO respectively, which for larger sizes represents the bandgap between valence and conduction bands). The same methodology can lead to the formation of stable and naturally abundant molecules (or crystals) from totally unstable or elusive molecules, such as the various triangulenes. The central idea is to (chemically or mechanically, e.g. with the STM tip) remove the "empty" (non-aromatic) peripheral rings, as is described below. The examples of molecular pairs such as circum-coronene (CIRCO) and hexabenzocoronene (HEXCO), or of extended 4-triangulene and 1, 3, 5-triphenylbenzene are highly suggestive that our "truncation" process could be a natural process; not just a conceptual one. This would be very important, intriguing, and illuminating. In what follows, the theoretical and calculational framework is reviewed and summarized in section 2. In section 3, the results and discussion for hexagonal (3.1) and triagonal (3.2) NGRs are presented, separately for armchair (3.2.1), and zigzag (3.2.2) structures. The main conclusions of the present work are summarized in section

4. Finally, a summary of the methods used is given in section 5. Additional information is included as supplementary information (SI).

2. Theoretical Framework. The customary concepts and computational tools used for the description of PAHs and NGRs are based in the fundamental ideas and rules of Kekulé in conjunction with the properties of alternant (or bipartite) hydrocarbons, using either the tight-binding (TB) model, or the more sophisticated one-orbital Hubbard model (in the mean field approximation), supplemented in many cases by chemical graph theory.[8-10] The key concepts of chemical graph theory are the sublattice imbalance expressed by the number N_A-N_B (the difference in the total number of sublattice sites A and B; and the nullity η, which is defined topologically as the difference between the maximum numbers of non-adjacent vertices and edges respectively).[8-10] For the high symmetry structures examined here, PAHs and NGRs, in which at most one sublattice is topologically frustrated, η is equal to the lattice imbalance, $\eta=|N_A-N_B|$, although in other cases, where both sublattices are frustrated,[8] η could be nonzero even when$=|N_A-N_B|=0$, as in the case of Clar's goblet.[7-8] Within the tight binding (TB) approximation, with the TB Hamiltonian, H_{TB} or H_0 including only nearest neighbor interactions η is equal to the number of nonbonding zero-energy states. This is also true for more advance models, such as the Hubbard model which includes (on-site) electron correlation (through the "Hubbard U"), such non-bonding states can get polarized, and in this case η also represents the number of singly occupied spin polarized states. The simplest one-orbital Hubbard model in the mean field approximation (see averages < > below), is described by the Hamiltonian

$$\left\{\begin{array}{l} H = H_0 + U\sum_i n_{i\uparrow} < n_{i\downarrow} > + < n_{i\uparrow} > n_{i\downarrow} \quad , \\ H_0 = -t\sum_{i,\mathrm{j},\sigma} c_{i\sigma}^{\dagger} c_{j\sigma} + c_{i\sigma} c_{j\sigma}^{\dagger} \end{array}\right\} \quad (1)\ ,$$

where H_0 is the usual TB Hamiltonian ($H_0 \equiv H_{TB}$) with t ($t \approx 2.7$ eV) the hopping integral and $c_{i\sigma}^{\dagger}, c_{i\sigma}$ the creation, annihilation operators, respectively, which create and annihilate an electron at site i with spin σ. U is the on-site Coulomb interaction, and $n_{i\uparrow} = c_{i\uparrow}^{\dagger}, c_{i\uparrow}$ and $n_{i\downarrow} = c_{i\downarrow}^{\dagger}, c_{i\downarrow}$ are the number operators at site i with spin up and spin down respectively. The mean field one orbital Hubbard model, despite the simplifying assumptions is still very much computationally demanding[8-10], and the results depend on the choice of the parameter U/t. Here instead we use a full quantitative description based on series of density functional theory (DFT) calculations in a well-defined sequence of PAHs and NGRs (together with judicially chosen isolated NGRs, when and where is required), supplemented by simple topological arguments of symmetry and aromaticity emerging from the shell model.[1] Such approach has been shown to indirectly include some key characteristics of the many-body theory description (of the electron-electron interaction)[1-3], and in particular some consequences of inversion symmetry frustration in the sublattice symmetry group, which is based in the notion of pseudospin (where as usual pseudospin up means sublattice site A, and pseudospin down is equivalent to sublattice site B). It is important to recognize that the formalism of eqs. (1) described above, could be also considered (with obvious minor modifications) as describing the pseudospin (instead of real spin). Therefore, Lieb's theorem[8] and other important conclusions based on it should be valid for pseudospin, entering (directly or indirectly) the present theoretical framework. Pseudospin or sublattice symmetry, which is a manifestation of chirality, is one important cornerstone of the present theoretical framework; the second is aromaticity (in its simplest geometrical notion). The concept of symmetry in Chemistry is not totally geometrical because seen as a mathematical point, a carbon atom with a lone pair or with an unbalanced number of (Kekulé-type) bonds, which is "topologically frustrated", like

in Clar's goblet,[7-8] is not Chemically "equivalent" to another carbon atom with normal balanced bonding. Likewise, carbon atoms with different environment or "chirality", belonging to different sublattices, are not (chemically) equivalent. Aromaticity, on the other hand, which is an extremely important and useful property, is often considered as a very "complicated", misunderstood, or redundant concept, largely controversial.[11-13] Most of the confusion arises not only from the fact that aromaticity is not a measurable quantity (which, however is common to many key properties in Chemistry), but mostly, according to Hoffman,[11] from various, sometime obscure, extensions of the original concept of aromaticity (which basically means "like benzene"), and a rather large number of aromaticity types, indices and criteria. In several cases such plethora of aromaticity indices could be conflicting with each other, although each one of these could serve a specific purpose.[12-13] Nevertheless, the simple and basic notion of aromaticity, as is adopted and applied here (requiring minimal basic knowledge, but no special or advanced aromaticity concepts and methods), is proven[1-3,15-16] an extremely useful, simple, powerful, and insightful "everyday" tool (see Computational Methods below). The central concept here is the "aromaticity pattern" i.e. the spatial distribution of aromatic (or "full") and non-aromatic (empty) rings. It is evident that in any polycyclic system (PAH, NGR, etc) not all the rings could be aromatic because the carbon atoms which "donate" the π-electrons belong to more than one (usually three) adjacent rings. The aromaticity pattern is pictorially described here by full red dots at the centers of the aromatic rings, which are also known as "full" rings. It can be shown[1-3] that due to symmetry (and shell structure) there could be only two types of aromaticity patterns, for fully developed structures with well-defined symmetry, vide infra. Using NICS(1) index for PAHs and NGRs of well-defined symmetry we find that the distribution of full (and, therefore, of empty as well) rings , which is governed by the

two fundamental (but empirical) rules of Hückel (demanding 4n+2 π-electrons for a cyclic ring), and Clar's rule of sextets[17] (6n π-electrons), are fully integrated and interrelated, or even fully coinciding, within the shell model,[1] which is materialized through a sequence of PAHs, consisting of n layers (or geometrical shells),with a benzene "nucleus" surrounded by n-1 annulenes rings (a total of n shells) one inside the other like a Russian babushka doll. These PAHs, the first 6 of which are shown in Fig. 1(a), constitute the "main sequence" of PAHs which serves as a bridge from benzene and Graphene, as more and more shells are added in the limit $n \rightarrow \infty$, where n is the "shell number". Although this sequence was invoked for describing the electronic (and in particular the aromatic) properties of Graphene[18], (which is the final end of the bridge), in the present study not only the end (graphene) is considered important, but the route itself (the main-sequence PAHs, and its derivatives) which sometimes, especially in the realm of poetry, could be even more important than the "end", as in the famous poem "Ithaka" by the Greek poet Kavafy (see also the caption of Fig. S1 in SI)! We can observe in Fig. 1(a), that all PAHs of the main sequence (with possible exception of benzene and coronene) are zigzag PAHs, although zigzag edges have been "demonized" as peculiar and non-aromatic. This is because isolated zigzag bonds, in contrast to armchair ones, violate the bipartite or "sublattice" symmetry and balance. Likewise, topologically frustrated, and "elusive" structures, which are best candidates for non-conventional magnetism[7-10] are almost invariably zigzag terminated. This last category of structures, which violates the fundamental bonding rules of Kekulé[6-8] (and Clar's as well), corresponds in the present scheme (of aromaticity patterns) to frustrated or "irregular", and/or "faint" aromaticity patterns characterized by very low (or zero) NICS(1) value(s)

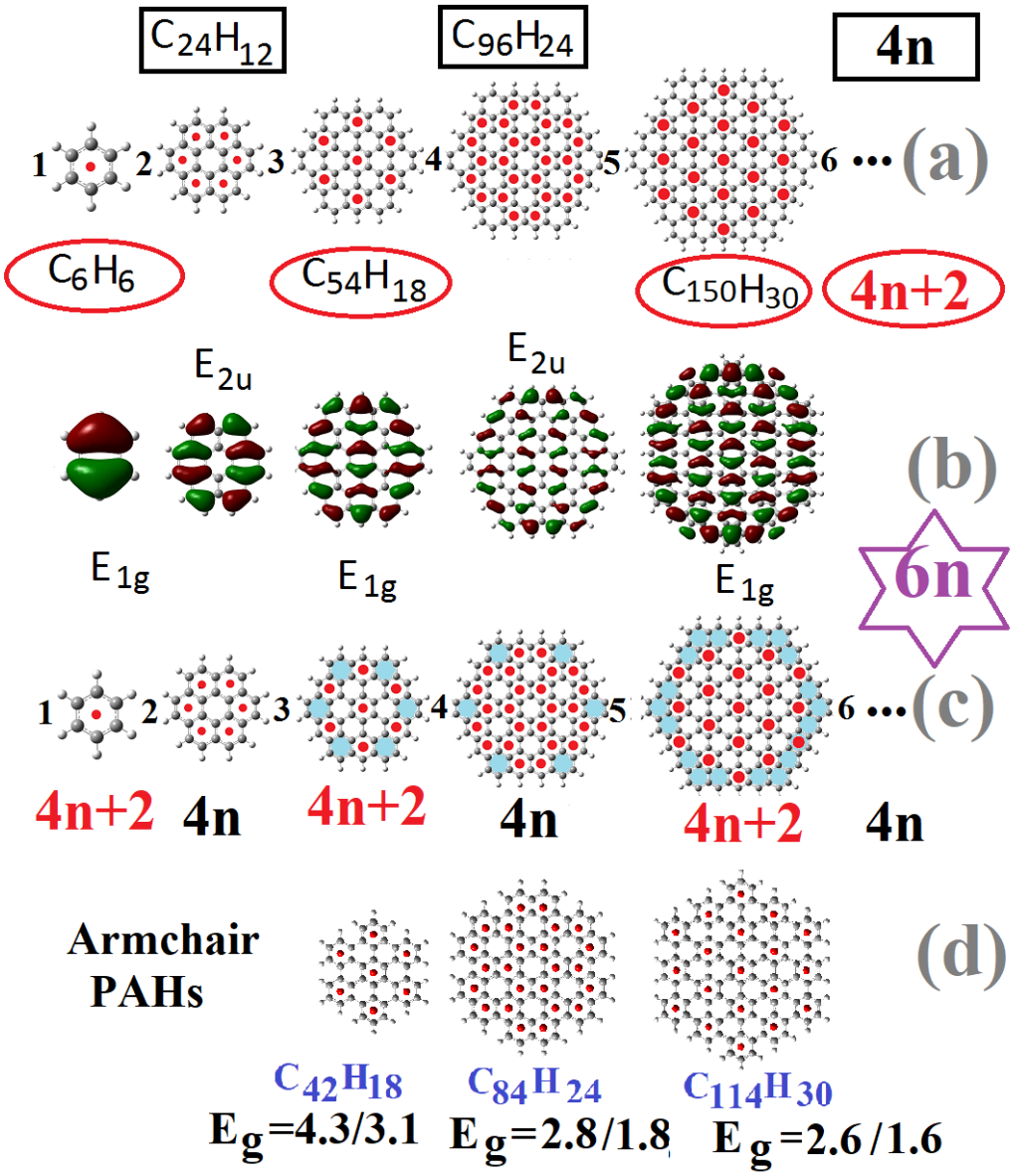

FIGURE 1. The first five members of the "main sequence" with their stoichiometry, aromaticity patterns, and "Hückel count" in **(a)**; HOMO orbitals and their symmetries in **(b)**; illustration of the ring-elimination process by showing empty peripheral rings, highlighted with light blue colour, in **(c)**; and the resulting armchair PAHs (with their aromaticity patterns, stoichiometry, and HOMO-LUMO gaps (E_g), in comparison to the parent PAHs) in **(d)**.

Nevertheless, neither the shell model nor Clar's or Hückel's rules directly distinguish between armchair and zigzag bonds and there is no direct relation (positive or negative)

between zigzag rings and aromaticity. Here such a direct relationship is finally established (*vide infra*). The starting and central point of the present work is the shell model defined by the main sequence[1], which incidentally is not just an abstract construction, but includes several concrete and well-known and well-studied PAHs, such as coronene (CO) and circum-coronene (CIRCO). In Figure 1(a) we can verify that there are (only) two alternating aromaticity patterns as n increases: one hexagonal as in coronene (CO-type), consistent with molecular symmetry, for even shell numbers n; and one trigonal for odd shell numbers, consistent with sublattice symmetry, as in circumcoronene (CIRCO-type). Such alteration of aromaticity patterns can be easily understood from the fact that each layer (annulene ring) addition, reflected in the *l*=n-1, shell number[1], is topologically equivalent to a rotation of the principal (x, y) axis by 60^o (characteristic of hexagonal symmetry)[2]. Thus, PAHs from Fig. 1 or S1 with an odd shell number n correspond to an even number of 60^o rotations, which is equivalent with an integer number of 120^o rotations, and hence with triagonal symmetry, reflected in the CIRCO pattern associated with even parity HOMOs, e_{1g} in Fig.1(b). This is because the parity of HOMOs[1] (representing the valence band in the limit $n\rightarrow\infty$) is $(-1)^{(n-1)}$, whereas for LUMOs is exactly the opposite, $(-1)^n$ (odd, e_{2u}). For the next n value this is reversed. Thus, the odd n PAHs with CIRCO aromaticity pattern are in full accord with Clar's rule of sextets (6k electrons),[1,17] which reflects triagonal symmetry. In addition, the same PAHs also satisfy Hückel's rule of 4m+2 π-electrons, and therefore in this case we could symbolically (and emphatically) write $6n=4n+2$ as in the title (where n in this relation is not the shell number n), meaning in fact: 6k=4m+2), k=1, 2,… (2). Since the number of π-electrons in the PAHs of the main sequence[1] is $6n^2$ (thus $k=n^2$), for odd values of the shell number we can write: $n=2\lambda+1$, and then for a given value of

λ=0, 1, 2, 3, … (i.e. n=1, 3, 5, 7, …), we can get the value of m from eq. (2): $m=6\lambda^2+6\lambda+1$ (3), resulting in m = 1, 13, 37, 73, …

For the PAHs with even shell-number eq. (2) cannot be satisfied and neither Clar's nor Hückel's rule are obeyed, although within each shell-ring separately, Hückel's rule (which is strictly valid for cyclic rings) is satisfied.[1] This is obviously true for the outer valence shell, thus explaining the arbitrary application of Hückel's rule in the past, selectively only to the outer periphery of PAHs. Thus, formally the failure of Hückel's rule can be alleviated by considering each shell separately (as the present author has suggested[1]), leading to a "generalized Hückel's rule", which is fully obeyed, explaining among others the well-recognized aromaticity of Coronene (corresponding to n=2). To compromise the "failure" of Clar's rule (and rationalize the aromaticity of the corresponding even-n PAHs (coronene in particular), the concept of migration of sextets was introduced to justify building the total wave function (or the total hexagonal aromaticity pattern) as a combination of two suitable trigonal structures (groups of rings) of D_{3h} symmetry, obeying Clar's rules and "sublattice" symmetry as well. Thus, for odd n (i.e. for even n-1) the molecular group could be also considered as D_{3h}, same as the sublattice group and the CIRCO aromaticity pattern, which is not possible for even n. Finally, we can observe in Fig. 1 (a), and (better) in Fig. S1, that the internal empty rings of one PAH become the full rings of the next, so that the pattern of the empty rings is complementary to the pattern of full rings (i.e. the aromaticity pattern). This is equivalent, as could be expected, to the complementary interrelation of the HOMO and LUMO orbitals in successive PAHs, which eventually ($n\rightarrow\infty$) are coupled at the Dirac points.[1-2] Thus, the full rings of the n PAH are the empty rings of the n-1 PAH, and its empty rings are the full rings of the n-1 PAH plus some additional empty rings in the periphery. It is tempting (and perhaps highly suggestive) to try to remove

these additional empty rings in the periphery, which in Fig. 1(c) and Fig. S1, are highlighted with light blue colour, preserving the hexagonal symmetry and saturating possible dangling bonds. The resulting (optimized) hexagonal structures after such "truncation" process are shown in Fig. 1(d). As we can see in Fig. 1(d) the resulting PAHs have the same shell number, the same aromaticity pattern, but "improved" armchair edges and higher HOMO-LUMO gaps by about 1 eV. It is therefore highly suggestive to apply this process to more cases.

3. Results and Discussion.

3.1 Hexagonal PAHs. The armchair PAHs in Fig. 1(d) have more in common with their zigzag parent structures beyond the aromaticity pattern, such as the structure and symmetry of the HOMO and LUMO orbitals, as is shown in Fig. S2 for HEXCO and CIRCO. These characteristics are invariant under the "truncation" transformation and are intimately connected with the shell number and the number of hydrogen atoms (although differently bonded), which are also invariant. Besides the obvious identity of the shell numbers (since the remaining peripheral rings belong to the same "valence" shell), the equality of the number of hydrogens follows, from the "effective shell number", which for hexagonal PAHs with incomplete shells (as HEXCO) is defined as the 1/6 of the number of hydrogens,[1] from the 6n hydrogens in the full-shell PAHs. of the main frequency. Thus, aromaticity patterns, shell number (effective or not) and symmetry of HOMO and LUMO orbitals, which are all interconnected remain invariant under truncation. Yet, although the aromaticity patterns are the "same" (the same rings are "full" before and after the "truncation"), the ring currents and the NICS(1) values could be lower, as is illustrated in Fig. S3 for the n=3 PAHs (CIRCO and HEXCO). The average NICS(1) value drops from -17.6 ppm in CIRCO to -12.1 ppm in HEXCO. This should be expected within the shell model[1] since the truncation process renders

the valence shell incomplete, but in a symmetrical way (i.e. keeping the hexagonal symmetry). For the corresponding electrons, this means that the 12 π-electrons removed, corresponding to the 12 carbon atoms eliminated, were distributed equally between MOs of positive and negative parity, as well as between nondegenerate and degenerate MOs, corresponding to 1-dimensional (1D), and 2-dimensional (2D) irreducible representations (2D) respectively, of the molecular symmetry group. Indeed, the missing electrons can be verified to have been taken out of the following configuration(s): $(b_{1g})^2(e_{1g})^4(a_{2u})^2(e_{2u})^4$, which fulfil the above conditions. Note that both CIRCO and HEXCO are stable and abundant, which is highly suggestive that such truncation transformation constitutes a natural process. In section 1.3 in SI, the balanced electronic configurations of the removed rings are also illustrated for the n=4, and n=5 PAHs. For example, the 36 removed electrons for n=5 belong to the configuration(s): $(b_{1g})^2(b_{2g})^2(e_{1g})^4\,(e_{2u})^4(e_{1g})^4\,(e_{2u})^4\,(a_{2u})^2\,(a_{1u})^2(e_{1g})^4(b_{1g})^2(e_{2u})^4(a_{2u})^2$, which are perfectly balanced (three odd 1D and 2D, and three even 1D and 2D representations). This guarantees the perfect similarity with the parent structure, which also includes bond-length distributions (see Fig. S4). Furthermore, in Fig. S5, is illustrated that the truncation process can be performed in more than one steps, provided each empty-peripheral-ring elimination preserves the hexagonal symmetry. Obviously, in this case, the intermediate structures are not expected to have the same degree of "perfection" as the final. For the n=6 PAH, the results shown for the n=6 PAH in Fig. S6, also emphasize the excellent HOMO, LUMO matching of the initial zigzag PAH $C_{216}H_{36}$ and the transformed armchair "homologous" hexagonal PAH $C_{180}H_{36}$. Finally, it is important to emphasize that the truncation process introduced here is a much more general process, well beyond the PAHs of the main sequence (and the hexagonal symmetry). In Fig. 2, especially in Fig. 2(b), this process is applied for the hexagonal

PAHs (with more than one geometrical open shells) $C_{252}H_{48}$ with a gap of 1.7 eV, which is gradually transformed by this process to the geometrically closed shell $C_{180}H_{36}$ PAH of the main sequence with n=6 (shown in Figs. 2(a) and S6) with a HOMO-LUMO gap of 2.1 eV. It is interesting to observe in this case, that the final structure does not have the same number of hydrogens (or effective shell number), but preserves the same aromaticity pattern, since the effective shell number changes by 2 units, keeping the same parity (even). Figure 2 also illustrates a different way of truncation in which only alternant groups of empty peripheral rings are eliminated. The resulting structures have triagonal (D_{3h}) symmetry, subgroup of D_{6h}, and are discussed in the next section.

3.2 Triagonal PAHs and NGRs

3.2.1 Armchair NGRs

The n=6 PAH in Fig. 2(a), shown also in Fig. S6, can be also transformed in an alternative ("alternating") way, as is shown in the upper part of Fig. 2 (a). Following the route (1) to (3), in the second row, instead of (1) to (2) in the first (top) row, we can delete every other group of empty rings, resulting in the triangular structure $C_{198}H_{36}$. This structure (3), $C_{198}H_{36}$, with (mainly) armchair bonds, following the same method of elimination, results in the all armchair bond structure (4), $C_{162}H_{36}$, with no empty peripheral rings (and, thus, "aromatically irreducible"). We can also observe that, although the parent hexagonal structure is characterized by a "Hückel count" of 4k and a "compatible" hexagonal CO aromaticity pattern, both triangular structures (3) and (4) have opposite "Hückel count" (4k+2), and "opposite" CIRCO aromaticity pattern. However, as we can verify in Fig. 2(b), and below in Fig. 3(a), the "Hückel count" is irrelevant for the outcome of such truncation process, but the triagonal CIRCO pattern and the armchair bonds are general and invariant characteristics for all of them.

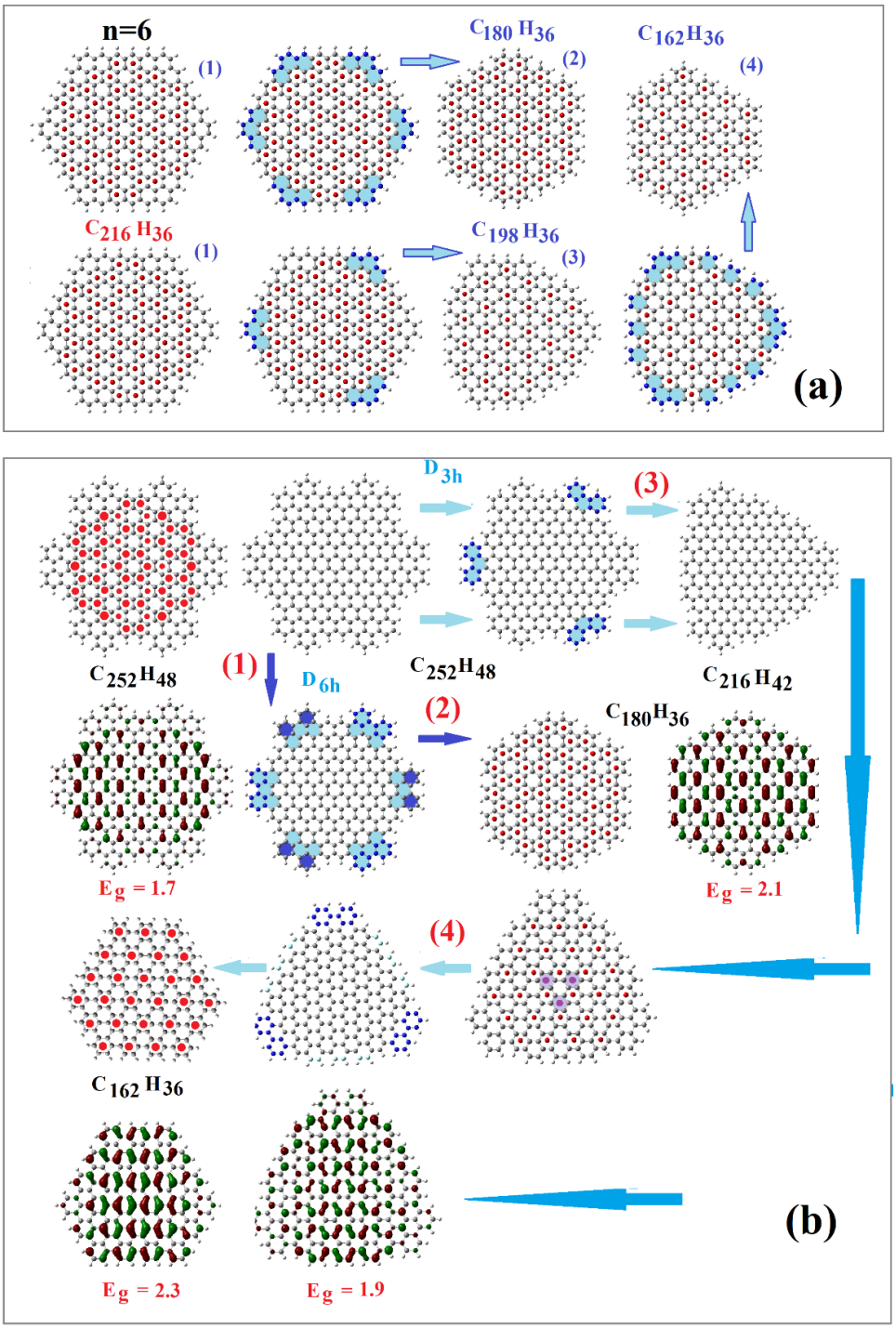

FIGURE 2. **(a)** The routes for the "closed shell" hexagonal (D_{6h}) zigzag PAH with n=6 to the "homologous" armchair PAH (with n_{eff} =6), (1)-(2), and to "daughter" D_{3h} PAHs, (1)-(3)-(4). Empty peripheral rings are highlighted with light blue color (on line). **(b)** Similar routes for the "open shell" n_{eff} = 8 PAH, including also initial, intermediate, and final HOMO

orbitals and HOMO-LUMO gaps (E_g). Dark blue highlighting emphasizes D_{6h} versus D_{3h} eliminations, whereas purple highlighting indicates "anomalous" rings (see text).

This can be understood from the fact that in this case the molecular and the (sub)lattice symmetry groups are the same (D_{3h}) with no inversion symmetry, and therefore no symmetry conflict (which was the underlying reason for the frustration and the "generation" of the CO pattern) and the Dirac points[2-3]. For the same reason both HOMO and LUMO orbitals have the same (e") symmetry, as can be seen at the bottom part of Fig. 2(b) and Fig. 3(a) below. The intermediate triagonal structure (4) with stoichiometry $C_{216}H_{42}$ (which also has a "Hückel count" of 4k, not 4k+2 as the other triagonal structures in Fig. 2) is characterized by an anomalous triagonal aromaticity region (shaded in the figure, apparently related with the remaining zigzag bonds), which disappears after final ring removal (step 4 in Fig. 2b). Furthermore, we can see (in Fig.2a) that the number of Hydrogen atoms at the edges during the $D_{6h} \rightarrow D_{3h}$ transformation remains the same. However, as we can also verify in Fig. 2(b), this is true for closed shell (geometrically/topologically) D_{6h} PAHs[1] or other "aromatically irreducible", e.g. all armchair D_{6h} structures. As was mentioned earlier for the geometrically/topologically open-shell PAHs, as $C_{252}H_{48}$, this is not true (neither for the intermediate D_{3h} structure (4), which is not all chair-bond bonded and "reducible aromatically"). In contrast, the (aromatically irreducible) $C_{162}H_{36}$ D_{3h} PAH, preserves the number of hydrogens (and therefor the "shell number") with the ("aromatically irreducible") $C_{180}H_{36}$ D_{6h} structure. Most of the conclusions drawn from Fig. 2, are verified and "fortified" in Fig.3. Figure 3(a), which is the triangular analogue of Figs. 1(a) and S1, shows the analogous triangular "main sequence"[1] as the corresponding "shell index" runs up to 6. As we can verify, all triangular PAHs of the main sequence are armchair bonded at their edges, have no empty peripheral rings (therefore they can be characterized as "aromatically

irreducible") and have exactly the same CIRCO aromaticity pattern, irrespectively of the number of π-electrons (number of carbon atoms) and (apparently) of the "Hückel count". Furthermore, there is no alteration in the symmetry of the HOMO, LUMO orbitals of a given PAH, neither between the HOMO's of successive PAHs, as in Fig. S1, due to the absence of inversion symmetry. Thus, both HOMO and LUMO are topologically identical, having the same e'' symmetry. As was explained above, this is a consequence of the coincidence of the molecular and (sub)group symmetries. As a result[2-3], there should be no Dirac points in such PAHs, and their properties would be expected to be different from those well-known properties of graphene-like PAHs (and graphene itself) , especially those directly related with Dirac's points. Therefore, no edge states should be present inside the gap[19]. This is partially reflected in the variation of HOMO-LUMO gap in Fig. 3(b), which shows much larger gaps (for a given shell number) from both zigzag and armchair hexagonal PAHs. This should be related to their "correct" aromaticity pattern, and to some extend to quantum confinement due to the smaller size of triangular NGRs for a given shell number (although the number of electrons could be smaller as well). Thus, although triagonal armchair nanographenes could be very efficient for appreciable bandgap opening (especially in view of the absence of topological edge states around the Fermi level), they would not expected to have the exotic properties of graphene and other NGRs, which are related with Dirac's points. Finally, we can observe in Fig. 3(b) that hexagonal armchair PAHs, contrary to the other two categories (Hexagonal zigzag and triagonal armchair) which show a smooth variation of the HOMO-LUMO gap in terms of the shell number, show clearly higher gaps for odd shell numbers, i.e. for PAHs satisfying both Clar's of sextets and Hückel's rules of 4n+2 π-electrons, compared to those of even shell number, suggesting higher aromaticity for the odd-shell-number PAHs.

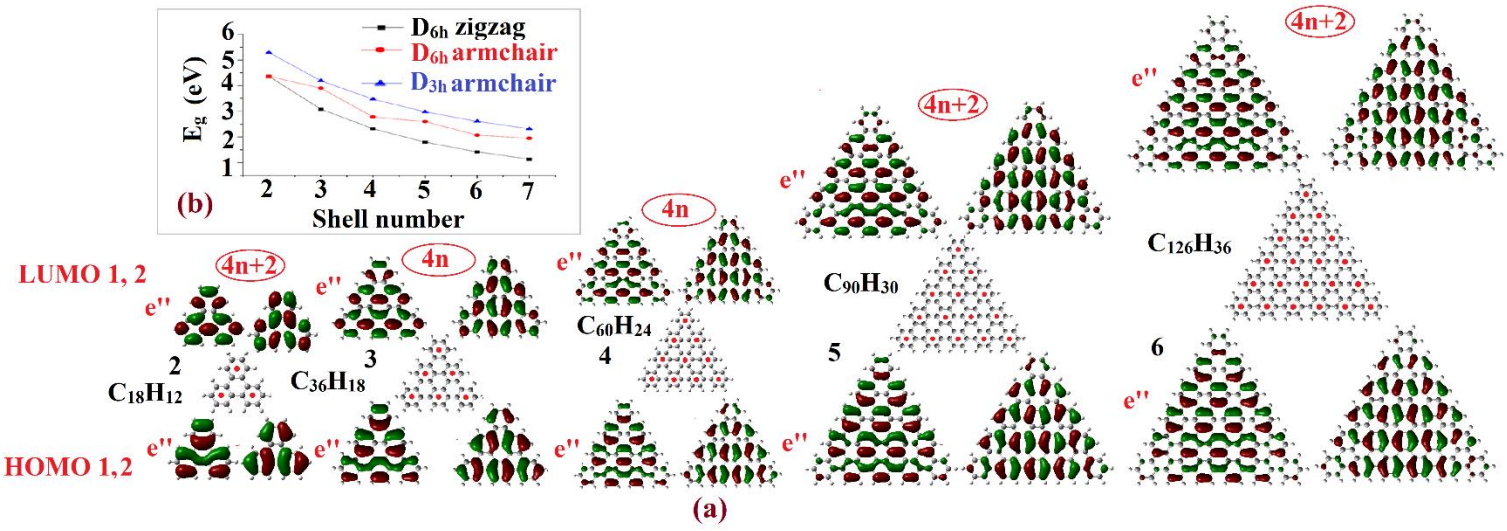

FIGURE 3. (a): A triangular version of the main sequence of PAHs[1], their aromaticity patterns, and their doubly degenerate e'' HOMO (1,2), LUMO (1,2) frontier orbitals in analogy to the hexagonal main sequence, for n=2-6; including, stoichiometry, "Hückel count" (4n, 4n+2), and "shell number" (see text). **(b)**: HOMO-LUMO gap (E_g) variation in terms of "shell number" for: hexagonal zigzag (black), hexagonal armchair (red), and triagonal armchair (bleu) PAHs.

3.2.2 Zigzag NGRs Contrary to armchair triagonal NGRs, zigzag triangular NGRs, not only are not aromatic, but they are topologically frustrated unstable and highly reactive open shell states, with (high) spin, depending on their size, due to inherent sublattice imbalance leading to unpaired electrons. In the aromaticity pattern picture adopted here, as we can see in Fig.4, this corresponds to very low aromaticity indices, such as NICS(1). Such structures clearly violate both Hückel's and Clar's rules, as is illustrated in Fig. 4 (*e.g.* by adjacent "full" rings). As a result, the NICS(1) values obtained (and displayed in Fig. 4) are very small with an average value around -6 ppm (compared to about -11.5 ppm for benzene), with the largest absolute value (-7 ppm) for the 2-triangulene ($C_{13}H_9$) in Fig. 4(a), which is actually a borderline case with practically armchair bonds. Despite their topological frustration and high

reactivity these triangulenes have been recently synthesized by novel techniques. The 3-triangulene was "synthesized" by manipulating physically atoms on individual molecules using the tip of a scanning tunnelling microscope (STM)[4]. The extended 4- and 5- triangulenes were synthesized by precise bottom-up synthesis using suitable molecular precursors on metallic surfaces.[4, 5] Looking at Fig.4, we can observe in the right portion of Figs. 4(b) and 4(c) that in both (and all) these cases the truncation process of eliminating "empty" peripheral rings, leads to better (larger absolutely) values of the average NICS(1) values, and lower spin values (by tree spin units), which are connected with the lattice imbalance N_A-N_B. Thus, the resulting structures have reduced (or none) lattice imbalance and smaller degree of topological frustration, and consequently better stability. For example, it is important to observe that, although the 4-triangulene is characterized by N_A=25, N_B=21, and N_A-N_B=4, with spin 4/2=2, the aromatically reduced structure $C_{24}H_{18}$ on the right portion of Fig. 4(b) is characterized by N_A=12, N_B=12, and N_A-N_B=0, with spin 0, without topological frustration, a large 5.1 eV HOMO-LUMO gap, and a large absolute value of average NICS(1) equal to -9.85 ppm (-8.2 ppm for the central ring and -10.4 ppm for each peripheral ring) close to the value for benzene. Moreover, the planar D_{3h} $C_{24}H_{18}$ structure is found not to be the global (or local) minimum of the energy hypersurface since it is characterized by a doubly degenerate e'' mode of imaginary frequency. However, when the planar structure is distorted according to the imaginary frequency mode, turns into a very well-known stable and naturally abundant structure of C_2 symmetry (in which the peripheral benzene rings are not in the same plane as the central ring). This is 1, 3, 5-Triphenylbenzene, with an extra stability of 0.33 eV in total energy, and a calculated HOMO-LUMO gap of 5.5 eV, which a very stable, and abundant molecule well-known both in the molecular and crystalline phase.[20] This illustrates the (unexpected) efficiency and consistency of this process, on top of its transparency and simplicity.

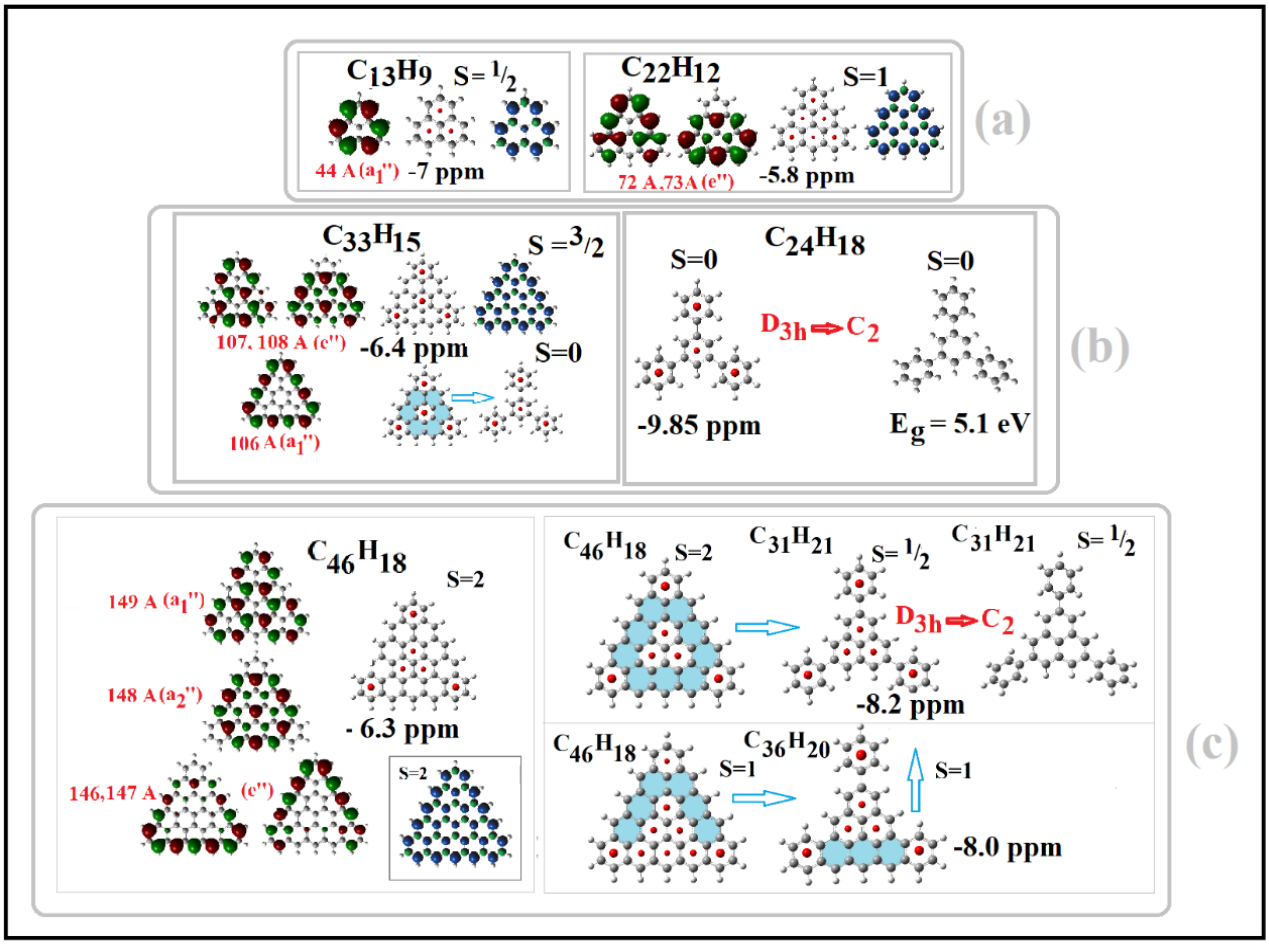

FIGURE 4. Electronic, Aromatic, and topological properties of the 2-, 3-triangulenes $C_{13}H_9$, $C_{22}H_{12}$ (a); 4-triagelene $C_{33}H_{15}$ (b), and 5-triangulene, $C_{46}H_{18}$ (c); including SOMOs (isovalue =0.2), with spin and space symmetry and orbital number; aromaticity patterns, and spin density (isovalue=0.004). Aromaticity patterns, based on the NICS(1) number (the average value of which, <NICS(1)>, is shown in ppm), are described by indicating the "full" (or not entirely empty) rings with red dots on their centers. For the 4- and 5- triangulenes the truncation process of the "empty" peripheral rings (highlighted by light blue colour on line) is also described in the right portion of Figs. 4(b), and 4(c), respectively (see text).

Moreover, in view also of the example of the aromatic pairs of circumcoronene and hexabenzocoronene, seen earlier, one could suggest that the "truncation process" uncovered

here could be not just a conceptual and efficient physicochemical tool, but a natural process as well. Such possibility is very intriguing, rendering special significance and importance in the present results. A similar process for the 5-triangulene ($C_{46}H_{18}$), as is illustrating in the right part of Fig. 4(c), leads first to the D_{3h} planar $C_{31}H_{21}$, with lattice imbalance N_A-N_B=1 and spin ½ (lower by 3 units, as before), and finally to the C2-symetric isomer which could be characterized as the three-phenyl substituted 2-triangulene (in Fig. 4(a), left portion). In the bottom line in the right part of Fig. 4(c), we can see a different form and version of the partial elimination (illustrated in Fig.2). If we choose the parent (5-trangelene) structure with the wrong spin, 1 instead of the correct 2, the geometry optimization leads to a planar C_{2v}-symmetric structure with full and empty rings as shown in the Figure (bottom right of Fig. 4(c)) $C_{36}H_{20}$, which following the next elimination process, leads again to the three-phenyl-substituted 2-triangulene ($C_{31}H_{21}$), as it should. This verifies emphatically the strong interrelation between topological (geometrical) and electronic characteristics, (electron spin in particular) for the triangulenes. This is in contrast to AGNR's zigzag ends,[3, 19] where the triplet-singlet energetical ordering is reversed when correlation is included, indicating that possible observed magnetism should be no conventional in the sense that it should not directly related with spin, but rather with pseudospin (i.e. rearrangement of p_z orbitals), [3, 19] . In triangulenes, as we can see in table 1, the triplet state is lower energetically before and after correlation (at the level of coupled clusters CCSD, with and without inclusion of perturbative triplet contributions (T), using the 6-31g(d) basis set), the inherent sublattice imbalance leads to open states with real spin and not pseudospin. This can be further illustrated for the 3-triangulene ($C_{22}H_{12}$), which with an even number of electrons (and atoms), is predicted (and verified) be open shell with spin equal to 1. This is consistent with the lattice imbalance N_A=10, N_B=12 ($|N_A-N_B|$= η= 2, S=η/2=1). The nullity η gives

the number of zero eigenvalues in the TB Hamiltonian, which in turn is equal to the number of singly occupied molecular orbitals (SOMOs).

TABLE 1. 3-Triangulene. Comparison of the Total energies of singlet and triplet states.

Method	**Singlet Energy (hy)**	**Triplet Energy (hy)**	**Triplet-Singlet (eV)**
DFT/PBE0	-844.5901863	-844.632982	-1.164
HF	-840.0612321	-840.228858	-4.559
CCSD	-842.914112	-842.968228	-1.472
CCSD(T)	-843.0791947	-843.1054334	-0.714

The SOMOs for this and the other triangulenes are shown in Fig.4 (a, b, c), whereas the complete energetical structure of the orbitals around the Fermi level is shown in Fig. S8. As we can see in Fig. 4(a) the two SOMOs for this triangulene are not localized at the edges (apparently due to quantum confinement), neither the spin density, as is several times mentioned in the literature. However, looking at the higher (4-, 5-) triangulenes in Fig. 4(b, c), we can see that some (almost half) of the SOMOs are indeed localized at the edges. In the same figure we can also see that the larger values of spin density are located at the edges, on C atoms of one (the "majority") sublattice. Nevertheless, smaller values are also found in the interior where several SOMOs are (de)localized, forming the sublattice pattern (structure). This should be expected since the spin values are directly related with the sublattice imbalance. Similar results for the 6-triangulene are summarized in Fig. S9, following the same rules, guidelines, notation, and conclusions.

4. Conclusions. By using and enriching the shell model[1] and related simple aromaticity concepts it has been shown that:

1) Hückel's and Clar's rules of aromaticity are intimately interrelated and for hexagonal NGRs and PAHs with odd "shell number" they are equivalent, satisfied simultaneously; whereas for "even shell number" they both fail (without additional external assumptions such as the generalized Hückel's rule, and the migration of sextets).

2) We can functionalize the electronic and aromatic properties of PAHs and NGRs and increase the HOMO-LUMO gaps (bandgaps) by controlling the empty peripheral rings, which are intimately connected with the zigzag bonds, without altering the form and symmetry of the frontier orbitals and the corresponding aromaticity patterns.

3) By eliminating empty (non-aromatic) peripheral rings in hexagonal zigzag NGRs we get armchair NGRs with improved properties (larger band gaps)

4) Partial elimination under D_{3h} subgroup leads to triangular armchair NGRs with armchair bonds with one unique Clar-type aromaticity pattern, independently of shell-number, parity, and number of π- electrons.

5) Triangular nanographenes are shown not to be graphene-like, in the sense that they have no Dirac points, which are generated by the competition between molecular and sublattice symmetry, due to identical molecular and sublattice symmetries (D_{3h}). Thus, triagonal nanographens should be either fully (Clar) and uniquely aromatic with armchair-edges, or non-aromatic and "frustrated", with zigzag-edges and high (true) spin.

6) Applying the same strategy of truncation (elimination of empty peripheral rings) to zigzag triangular NGRs (triangulenes) we get more stable structures with smaller sublattice imbalance and spin, by 3 units. In the case of the extended [4]-triangulene, we finally obtain the 1,3,5-triphenylbenzene which is a stable naturally abundant molecule with closed shell structure (S=0), large (5.5 eV) HOMO-LUMO gap, and NICS(1) value close to benzene.

7) Based on paradigms of hexabenzocoronene and triphenylbenzene, it is suggested that this could be a natural (not just a conceptual or mechanical) process.

8) Finally, it is suggested that this process should be very useful for other graphene nanostructures for the manipulation (perhaps by STM tip methods) and functionalization of their structural, electronic, aromatic, and magnetic characteristics simultaneously.

Thus, further work on this subject (both experimental and theoretical) should be very important.

5. Computational Methods. The theoretical and computational framework of this work, which includes a multitude of systematic and interconnected (one-body) DFT calculations on PAHs, NGRs and GNRs (AGNRs) of given symmetry, has been discussed earlier,[1-2] together with the technical details. In the present work the "main sequence" of hexagonal PAHs, which defines the shell structure, has been expanded and extended to include analogous rectangular NGRs and GNRs (AGNRs), analyzed in terms of simple group theory and topological concepts and connections. All geometrical structures have been optimized (or reoptimized) using tight convergence criteria at the DFT level of the hybrid PBE0[21] functional using the 6-31G(d) basis set, as is implemented in the GAUSSIAN program package (G09)[22]. Similarly, the CCSD and CCSD(T) calculations were performed with G09. The same package was also used for the calculation of NICS(1) aromaticity index, which for the present work has been proven satisfactory and suitable[1-2, 15-16]. This level of theory, used consistently and uniformly for all structures small and large (for all related properties), is fully adequate for such calculations, as was pointed out earlier.[1-3, 13, 19] For the visualization of the results (orbitals, electronic and spin densities) the GaussView[23] program was used.

References

1. Zdetsis, A. D. Classics Illustrated: Clar's Sextet and Hückel's (4n+2) π Electron Rules. *J. Phys. Chem. C*, **2018**, 122, 17526-17536.
2. Zdetsis, A. D. Bridging the Physics and Chemistry of Graphene(s): From Hückel's Aromaticity to Dirac's Cones and Topological Insulators. *J. Phys. Chem. A* **2020**, 124, 976-986
3. Zdetsis, A. D. Do We Really Understand Graphene Nanoribbons? A New Understanding of the 3n, 3n±1 Rule, Edge "Magnetism" and Much More. *J. Phys. Chem. C* **2020**, 124, 7578−7584
4. Pavliček, N. *et al.* Synthesis and characterization of triangulene**.** *Nature Nanotechnol.* **2017,** 12, 308–311 DOI:10.1038/nnano.2016.305
5. Mishra, S. ; Beyer, D.; Eimre, K. *et al.* et al. Synthesis and characterization of *π*-extended triangulene. *J. Am. Chem. Soc.* **2019** 141, 10621–10625
6. Su, J.; Telynchko, M.; Hu, P. et al. Atomically precise bottom-up synthesis of *π*-extended [5] triangulene. *Sci. Adv.* **2019** 5, eaav7717
7. Mishra, S.; Beyer, D.; Eimre, K. *et al.* Topological frustration induces unconventional magnetism in a nanographene. *Nat. Nanotechnol.* **2020,** 15, 22–28
8. Wang, W. L., Yazyev, O. V., Meng, S. & Kaxiras, E. Topological frustration in graphene nanoflakes: magnetic order and spin logic devices. *Phys. Rev. Lett.* **2009** 102, 157201
9. Yazyev, O. V. Emergence of magnetism in graphene materials and nanostructures. *Rep. Prog. Phys.* **2010**, 73, 0565
10. Tucek, J.; Btonski, P.; Ugolotti, J.; Swain, A. K.; Enoki, T.; Zboril, R. Emerging chemical strategies for imprinting magnetism in graphene and related 2D materials for spintronic and biomedical applications. *Chem. Soc. Rev.* **2018**, DOI: 10.1039/c7cs00288b

11. Hofman R. The Many Guises of Aromaticity. *Am. Sci.* **2015**, 103, 18

12. Boldyrev, A. I.; Wang L.-S. Should Aromaticity Be Reserved For Only Benzene And Its Derivatives? Chem. & Eng. News online 2015, http://cenm.ag/aromatic

13. Sola, M. Why Aromaticity is a Suspicious Concept? Why? *Front. Chem.,* **2017**, 5, 22 .

14. Zdetsis, A. D.; and Economou, E.N. Electronic and aromatic properties of graphene and nanographenes of various kinds: insights and results, *Adv. Mat. Lett.* **2017**, 8, 256-261

15. Schleyer, P.v.R.; Maerker, C.; Dransfeld, A.; Jiao, H.; van Eikema Hommes, N.J.R. Nucleus Independent Chemical Shifts: A simple and Efficient Aromaticity Probe, *J. Am. Chem. Soc*. **1996**, 118, 6317–631

16. Sola, M.; Feixas, F.; Jimenez-Halla, J. O. C.; Matito, E; Poater, J. A Critical Assessment of the Performance of Magnetic and Electronic Indices of Aromaticity. *Symmetry*, **2010**, 2, 1156-1179

17. Clar, E. The Aromatic Sextet; Wiley: New York, NY, **1972**

18. Popov, I. A.; Bozhenko, K. V. ; and Boldyrev, A. I. Is Graphene Aromatic? *Nano Res.***2012**, 5, 117–123

19. Zdetsis A. D.; Economou, E. N. Topological Metal-Insulator Transition in Narrow Graphene Nanoribbons? , Chemarxiv, **2020** DOI: 10.26434/chemrxiv.12469607 ,v2.

20. Prasad, D.; Preetam, A.; Nath, M. Experimental Crystal Structure Determination. *CCDC* 867818. **2013** DOI: 10.5517/ccy4147

21. Adamo, C.; Barone,V. Toward Reliable Density Functional Methods Without Adjustable Parameters: The PBE0 model. *J. Chem. Phys.*, **1999,** 110 6158-69

22. Frisch, M. J.; Trucks, G.W.; Schlegel, H. B.; Scuseria, G. E.; *et al*., Gaussian 09, Revision C.01, Gaussian, Inc., Wallingford CT, **2009**.

23. GaussView, Version 5.09, Dennington, R; Keith, T; Millam, J. Semichem Inc., Shawnee Mission, KS, 2016.